
Strain Elastography Fat-to-Lesion Index Is Associated with Mammography Bi-rads Grading, Biopsy, and Molecular Phenotype in Breast Cancer.

[Jose Alfonso Cruz-Ramos](#)^{*}, Mijail Irak Trapero-Corona, Ingrid Aurora Valencia-Hernandez, Luz Amparo Gomez-Vargas, Maria Teresa Toranzo-Delgado, Karla Raquel Cano-Magaña, Emmanuel De la Mora-Jimenez, [Gabriela C. López-Armas](#)^{*}

Posted Date: 13 December 2023

doi: 10.20944/preprints202312.0916.v1

Keywords: Elastography; Breast Cancer; fat-to-lesion index



Preprints.org is a free multidiscipline platform providing preprint service that is dedicated to making early versions of research outputs permanently available and citable. Preprints posted at Preprints.org appear in Web of Science, Crossref, Google Scholar, Scilit, Europe PMC.

Copyright: This is an open access article distributed under the Creative Commons Attribution License which permits unrestricted use, distribution, and reproduction in any medium, provided the original work is properly cited.

Article

Strain Elastography Fat-to-Lesion Index Is Associated with Mammography BI-RADS Grading, Biopsy, and Molecular Phenotype in Breast Cancer

José Alfonso Cruz-Ramos ^{1,2,*}, Mijaíl Irak Trapero-Corona ², Ingrid Aurora Valencia-Hernández ³, Luz Amparo Gómez-Vargas ², María Teresa Toranzo-Delgado ², Karla Raquel Cano-Magaña ², De la Mora Jiménez Emmanuel ² and Gabriela del C. López Armas ^{4,*}

¹ Instituto de Patología Infecciosa y Experimental, Departamento de Clínicas Médicas, Centro Universitario de Ciencias de la Salud, Universidad de Guadalajara; Guadalajara 44340, México

² Instituto Jalisciense de Cancerología, Guadalajara, 44280, México

³ Departamento de Ciencias Computacionales. Instituto Nacional de Astrofísica Óptica y Electrónica, San Andrés Cholula, Puebla 72840

⁴ Laboratorio de Biomédica-Mecatrónica, Subdirección de Investigación y Extensión, Centro de Enseñanza Técnica Industrial Plantel Colomos, Guadalajara 44638, México; glopez@ceti.mx

* Correspondence: jalfonso.cruz@academicos.udg.mx (J.A.C.-R.); glopez@ceti.mx (G.d.C.L.A.)

Abstract: Breast cancer (BC) affects millions of women; it is the leading cause of death by neoplasia in women worldwide, with at least 500 thousand deaths each year, 70% of which occur in developing countries. Elastography evaluates tissue stiffness, making this a promising non-invasive real-time technique. BI-RADS is recognized as a standard and helpful technique for establishing BC risk. This study aimed to determine, by strain elastography (SE), the fat-to-lesion index (F/L index), sensitivity, specificity, and optimal cut-off to diagnose BC. This prospective study included 216 women who underwent SE, ultrasound, mammography, and breast biopsy; according to mammography, we recruited BI-RADS category 2 (n= 5), category 3 (n=29), category 4 (n= 94), category 5 (n= 71) and category 6 (n=17); after biopsy, 108 women were classified as negative, and 108 were positive for BC. Three expert BC radiologists performed all imaging interpretations and biopsies. Our results show mean values of the F/L index for negative biopsies of 3.70 ± 2.57 and positive biopsies of 18.10 ± 17.01 ; we developed two models for the prediction of BC, a logistic regression model with an AUC of 0.893 and a neural network with an AUC of 0.902. The Youden index yielded a F/L index cut-off >5.76 , with a sensitivity and specificity of 84.26%. Positive Spearman's Rho correlation coefficient was observed between the F/L index and BI-RADS, $r=.073$ ($p < 0.001$). ANOVA test showed a difference between F/L index vs. molecular subtypes ($p=0.002$). SE is helpful as a diagnostic complement to mammography, or in cases where the latter is contraindicated, elastography has an adequate predictive capacity and is a fast and minimally invasive procedure.

Keywords: elastography; breast cancer; fat-to-lesion index

1. Introduction

Breast Cancer (BC) is a major public health worldwide; until today, GLOBOCAN reports a prevalence of 7,790,717 females with BC in 2020[1]. In this sense, the most helpful tool for BC diagnosis is mammography and ultrasound (US) as a complementary test; this includes elastography, a non-invasive technique to address the biomechanical properties of the tissue measuring stiffness to evaluate the resistance to the passage of acoustic waves through the structures and tissues of the body (anisotropic, viscous, and nonlinear behavior[2]. Besides, elastography gives us an elastogram image to observe Young's modulus, Poisson's ratio, or the unitary deformations[3]. We can mention that elastography consists of two categories: semi-quantitative or strain elastography (SE) and

quantitative or shear-wave elastography (SWE)[4]. SE elastography obtains the elasticity of the tissues with the primary compression of the natural composition (fat) of the breast tissue before the deformation[5,6]. Then, another measurement is acquired by soft compression with the transducer by conducting the movement of the deformed breast tissue (mass) and is calculated in the same moment; then a radiologist compares these two measurements, and an SE gives as a result the fat-to-lesion index (F/L-index). Conversely, SWE evaluates tissue elasticity by calculating the shear wave propagation velocity. It does not require tissular pressure since it measures the displacement independently of the applied pressure and sends acoustic micro impulses with minimum energy levels to the different tissues; the elasticity is expressed in units of velocity in m/s or as the pressure in kilopascals (kPa)[7,8].

In general, elastography, either SE or SWE, has become, in the last 15 years, a tool with predictive value to determine whether a tumor is benign or malignant (e.g., liver, prostate, and thyroid)[9–11], particularly in the breast it takes more importance since US is a screening tool for the detection of breast tumors before the age ≤ 40 years or in women with small and dense breasts, where mammography may not have the same sensitivity[12,13]. Elastography is a technique widely recognized by the American College of Radiology in its latest edition[14]; this is derived from using the US to measure the hardness of the tissues; several papers have been published over time between tissue elasticity and its association with BC[2,15].

This work uses SE to show us color images or maps of consistent breast tissue. Also, we consider the strain ratio of fat-to-lesion (F/L) of the region of interest (ROI). This study aimed to determine F/L index sensitivity, specificity, and optimal cut-off to diagnose BC and benign tumors. Besides, we analyzed BI-RADS concordance, BC subtypes, clinical stages, and grading tumors.

2. Materials and Methods

This retrospective, transversal, and descriptive study was conducted in the Instituto Jalisciense de Cancerología (IJC), which involved all Occidental regions of Mexico. This study was sustained following the regulations of the General Health Law, the Regulations of the General Health Law on Health Research, the guidelines established by COFEPRIS, the Health Law of the State of Jalisco, the Ethics and Research Committee of the OPD of IJC with number register CONBIOETICA-14-CEI-004-20170421, and those established by the E6 Good Clinical Practice (GCP) Guide of the International Conference on Harmonization (ICH). All the patients gave written informed consent.

Patients

The data collection was from January 2017 to April 2023. The inclusion criteria were female patients aged 18 to 78, with a positive or negative solid lesion in the breast, through examination with B-mode US with SE and histological confirmation in all cases. One hundred and eight breast biopsies of patients were negative, and one hundred and eight were BC positive. All patients were paired according to age.

Ultrasound and Strain Elastography

In this study, all patients with any mass or suspicion of them were exposed to US exploration and SE; those studies were performed by 3 radiologists with more than 15 years of experience in breast imaging. All measurements and images were acquired with a Hitachi Avius (Hitachi Medical, Tokyo, Japan) equipped with a multifrequency linear transducer from 7 to 12 MHz, with color Doppler and elastography by placing the transducer on longitudinal scans. We use semi-quantitative elastography in all patients, measuring three times with slight compression according to the World Federation for Ultrasound in Medicine & Biology (WFUMB) Guidelines, obtaining a final average (Figure 1) [16]. All lesions were classified by the 5th edition of Breast Imaging Reporting and Data System (BI-RADS), where category 2 is benign, category 3 is probably benign, category 4 is suspicion of malignancy and is segmented in 4A (low suspicious for malignancy), 4B (moderate suspicious for

malignancy), and class 4C high suspicious for malignancy (in all of them, biopsy is required), and category 5 is highly suspicious for malignancy (biopsy mandatory)[17]

Primary care clinics and BC units referred to the IJC were reclassified through new mammography, B-mode ultrasonography, and elastography. Of all the cases, 50.9% were recategorized into BI-RADS; the data collected for the analysis were the BI-RADS assigned by the IJC radiologists.

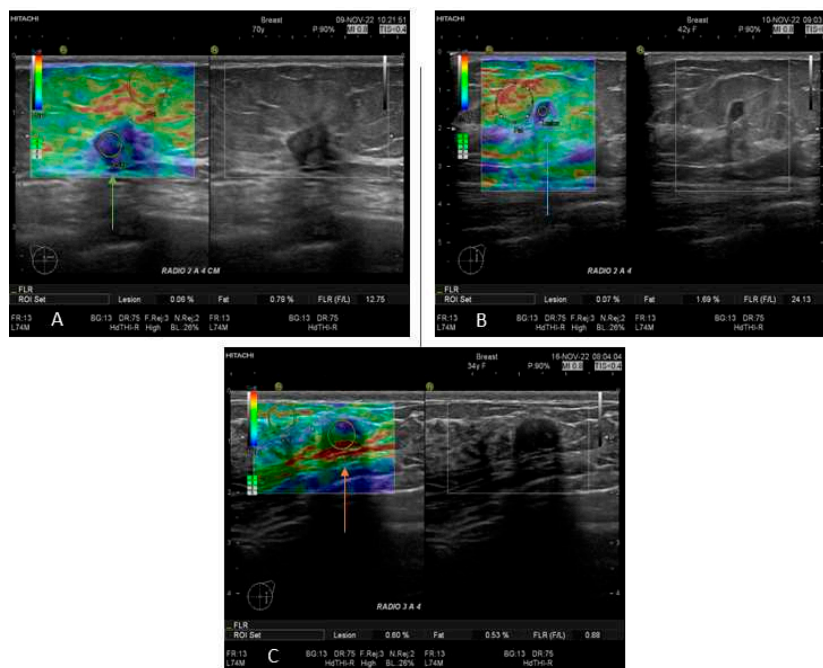


Figure 1. Images of B mode US and SE, corresponding to A) TN tumor in a female of 70 years old (green arrow) with F/L index 12.75; B) Luminal A tumor in a female of 42 years old (blue arrow) and C) Negative biopsy in a female of 34 years old (orange arrow).

Histological and Immunohistochemistry evaluation

After performing the elastography, all patients underwent a biopsy; the tissues were formalin-fixed and paraffin-embedded (FFPE) and stained with hematoxylin and eosin for classification tumors according to the WHO classification breast tumors and for histological features, the modify Scarf Bloom- Richardson (SBR) grading system was used; regarding immunohistochemistry (IHC) to determine the molecular subtypes of BC (Luminal A corresponding to ER+ and/or PR+, HER2-, and Ki-67 <14%, Luminal B corresponding to ER+ or PR+/-, HER- and either Ki-67 >14%, Luminal B-like corresponding to (ER+, HER2+, any Ki-67, and any PR), HER2+ corresponding to ER/PR-, and HER2+, and triple-negative (TN) corresponding to ER/PR-, and HER2-) according to the 2011 St. Gallen Consensus Conference, and 13th St. Gallen International Breast Cancer Conference [18,19], pathologists with over 20 years of experience in diagnosing breast tumors within the IJC examined all tissues for light microscopy.

Clinical Stages in BC

Patients in this study who tested positive for BC were subjected to appropriate surgical intervention. The clinical oncologist determined the clinical stage of the disease according to the Eighth Edition of the AJCC Cancer Staging Manual: Breast Cancer [20] in conjunction with the histopathological review of the histological grade and the molecular subtype of BC; with these data, the pharmacological behavior was standardized as appropriate; all clinical and surgical oncologists involved in this study have more than 10 years of experience.

Statistical Analysis

All data analysis and plots were performed by SPSS software version 25.0 (WPSS Ltd., Surrey, UK (accessed on 15 November 2023), JASP team (2023) JASP version 0.18.1.0) computer software (accessed on 15 November 2023) and GraphPad Prism version 9.02 for windows (accessed on 15 November 2023), quantitative data were represented as means and standard deviation; qualitative data as frequencies or percentages. Normality was performed by the Shapiro-Wilk test.

Inferential analysis was made with Student's t-test and ANOVA for normal distribution and Mann's U-test, Kruskal Wallis test for non-normal distribution, and Spearman's rho correlation was applied. Chi-square or Fisher's exact test was used for qualitative data. Principal Component Analysis (PCA) was used to summarize features for better insight. Subsequently, the significant variables ($p < 0.05$) were selected and included in a multivariable logistic regression model and neural network analysis, which were evaluated using the ROC curve and the Akaike criterion.

For neural network analysis settings, we implemented a multilayer perceptron neural network with a fixed seed of 2 million, 2 thousand epochs, and two hidden layers; both activation functions for the hidden layer and output layer used the hyperbolic tangent.

3. Results

A total of 216 patients were included in this study. The mean age of women with malignant biopsies was 51.38 ± 10.80 years old; in contrast, the mean age of patients with benign biopsies was 50.64 ± 10.81 years old. The average value of tumor diameter in patients with negative biopsy was 16.88 ± 12.86 mm, compared to patients with positive biopsy, which was 24.20 ± 17.67 mm. The F/L index mean value was 3.70 ± 2.57 for benign lesions; meanwhile, for malignant lesions, the average value for the F/L index was 18.10 ± 17.01 (Table 1).

Table 1. Descriptives for age, diameter, F/L index, and normality test.

Descriptives statistics	Age		Diameter		F/L INDEX	
	Neg	Pos	Neg	Pos	Neg	Pos
Biopsies result						
Median	49.50	50.00	14.00	24.00	2.96	11.66
Mean	50.64	51.38	16.88	24.20	3.70	18.10
SD	10.81	10.80	12.86	17.67	2.57	17.01
P-value of Shapiro-Wilk	0.18	0.61	< .001*	< .001*	< .001*	< .001*

SD: Standard Deviation; Neg: Negative; Pos: positive; Shapiro-Wilk test for normality; * p-value significance <0.05.

3.1. Principal Component Analysis

Principal Component Analysis (PCA) was carried out to visualize and explain our main clinical features. After the analysis, we obtained two graphs, and both results manifested similar outcomes; patients who tested positive for malignancy tended to concentrate on the left quadrant, while patients who tested negative for malignancy focused on the right quadrant. On top of that, a higher F/L index and a larger diameter were prevalent on the left quadrant of both PCAs (Figure 2).

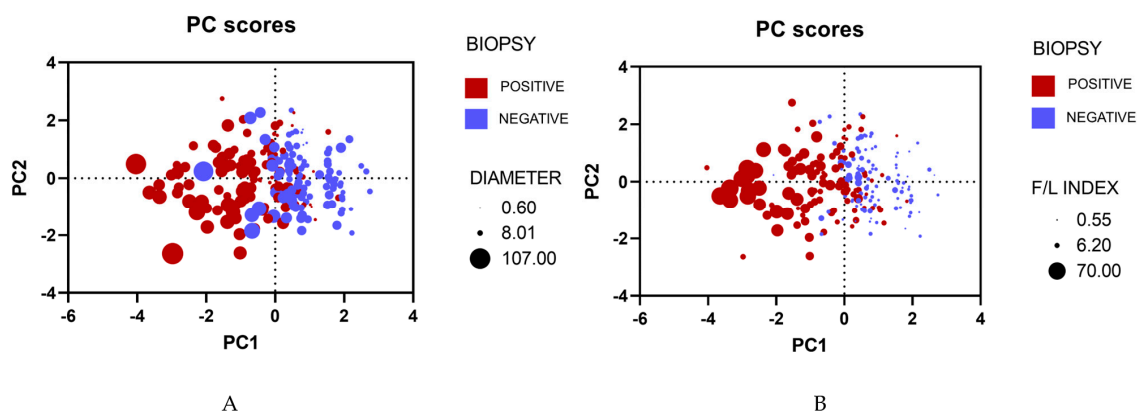


Figure 2. A) Principal Component Analysis of Biopsies and Diameter; B) Principal Component Analysis of Biopsies and F/L Index.

3.2. Histological type, BI-RADS Assignment

Among all the patients positive for malignancy, 94 patients were diagnosed with invasive ductal carcinoma (IDC) (87.04%), and 10 patients were detected with invasive lobular carcinoma (ILC) (9.26%). On the other hand, benign tumors fibroadenoma was predominant in 59 patients (54.63%), after fibrocystic changes in 9 patients (8.33%), ductal hyperplasia was present in 15 patients (13.89%), lobular hyperplasia in 1 patient (0.93%) and atypia in 2 patients (1.85%) were less common. Notably, cases without histological results were categorized as "Missing" (20.37%). Regarding BI-RADS classification, we observed a higher proportion of BI-RADS 5 (30.09%), followed by BI-RADS 4A (23.15%), BI-RADS 4C (14.81%), BI-RADS 4B (13.89%), and BI-RADS 3 (13.43%). BI-RADS 2 and BI-RADS 6 were less prevalent, accounting for 2.31% of all the cases. (Table 2)

Table 2. Frequency of clinical features.

Malignant tumors	N	Percent (%)
IDC	94	87.04%
ILC	10	9.26%
Missing	4	3.70%
Total	108	100.00%
Bening tumors	N	Percent (%)
Fibroadenoma	59	54.63%
Fibrocystic	9	8.33%
Ductal Hyperplasia	15	13.89%
Lobular Hyperplasia	1	0.93%
Atypia	2	1.85%
Missing	22	20.37%
Total	108	100.00%
BI-RADS	N	Percent (%)
2	5	2.31%
3	29	13.43%
4A	50	23.15%
4B	30	13.89%

4C	32	14.81%
5	65	30.09%
6	5	2.31%
Total	216	100.00%

IDC: Invasive ductal carcinoma, ILC: Invasive lobular carcinoma, BI-RADS: Breast Imaging Reporting and Data System.

3.3. Clinical stages, Grading tumors, and Molecular subtype BC

Additionally, in the malignancy tumors group, clinical stage III (38.89%) was more frequent, succeeded by stage II (34.26%), stage I (14.81%), and stage IV (9.26%). Moreover, the proportion of histological grade was the following: grade 1 or well-differentiated (1.85%), grade 2 or moderately differentiated (70.37%), and grade 3 or poorly differentiated (19.44%). Concerning molecular subtypes, we observed Luminal B (35.19%) and Luminal A (33.33%) in higher proportions, preceded by TN (15.74%) and finally HER2-enriched (11.11%) in less frequency (Table 3). We performed a Chi square with no significant results to compare clinical stages and molecular subtypes.

Table 3. Clinical features of malignancy tumors.

Stage	N	Percent (%)
I	16	14.81%
II	37	34.26%
III	42	38.89%
IV	10	9.26%
Missing	3	2.78%
Total	108	100.00%
Grade	N	Percent (%)
1	2	1.85%
2	76	70.37%
3	21	19.44%
Missing	9	8.33%
Total	108	100.00%
Molecular subtype	N	Percent (%)
HER2-enriched	12	11.11%
Luminal A	36	33.33%
Luminal B	38	35.19%
TN	17	15.74%
Missing	5	4.63%
Total	108	100.00%

N: Frequency, TN: Triple Negative, HER2: human epidermal growth factor receptor 2.

Our results demonstrated that the F/L index had a positive and significant correlation between BI-RADS classification ($r=0.73$) and tumor diameter ($r=0.35$); similarly, BI-RADS classification was positively and significantly correlated with tumor diameter ($r=0.40$) and clinical stage ($r=0.25$). At the same time, clinical stage and tumor diameter showed a positive and significant correlation ($r=0.21$) (Figure 3).

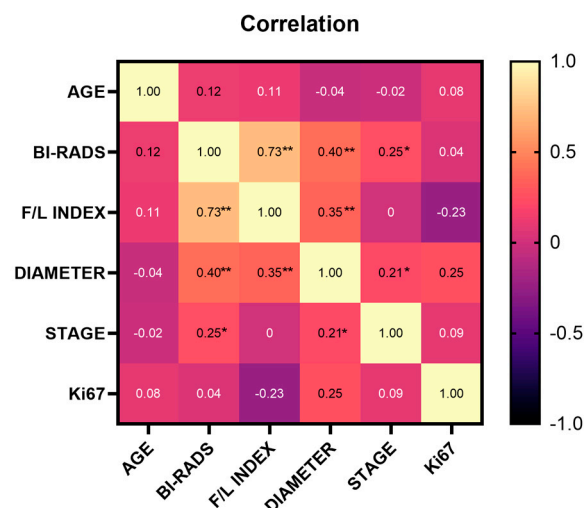


Figure 3. Spearman's Correlation matrix of variables of the study. The strongest correlations are marked with ** Significant correlation <0.01 (bilateral); *significant correlation <0.05 (bilateral).

Furthermore, we found a significant association between the F/L index and the tumor biopsy ($p < 0.001$). A lower F/L index was identified in malignancy-negative biopsies, as opposed to a higher F/L index in malignancy-positive biopsies (3.70 vs. 18.10). Figure 4A

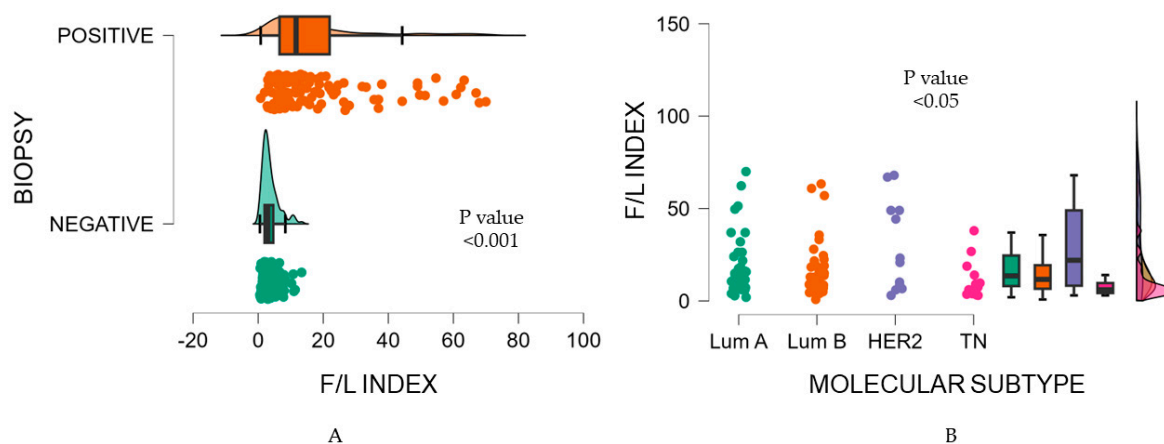


Figure 4. ANOVA test for A) biopsies and F/L index; B) subtype and F/L index.

Consequently, the ANOVA test showed the F/L index presented significantly different values within molecular subtypes classification ($p=0.02$) (Figure 4B); HER2-enriched showed a F/L index of 29.66 ± 24.42 , contrary to TN with an average F/L index of 10.15 ± 9.52 . Luminal subtypes disclosed similar values among them, with a mean F/L index of 19.34 ± 16.73 for Luminal A and a mean F/L index of 16.53 ± 15.35 for Luminal B, respectively (Table 4). Dunn's post-hoc test for intra-group comparisons, indicated a difference between Luminal A vs. TN and HER2-enriched vs TN; both findings were significant ($p < 0.05$ and $p < 0.04$) (Table 5).

Table 4. Descriptives Mann-Whiney U test. F/L INDEX vs Subtype.

Subtype	N	Mean	Median	SD	SE	Coefficient of variation
Luminal A	36	19.34	13.60	16.73	2.79	0.87
Luminal B	38	16.53	11.70	15.35	2.49	0.93
HER2-enriched	12	29.66	22.00	24.42	7.05	0.82
TN	17	10.15	6.08	9.52	2.31	0.94

TN: Triple negative, HER2: human epidermal growth factor receptor 2.

Table 5. Dunn's post-hoc comparison ANOVA test.

Intra-group comparison	P value
Luminal A – Luminal B	>1.00
Luminal A – HER2-enriched	>1.00
Luminal A – TN	<0.05*
Luminal B - HER2-enriched	>1.00
Luminal B – TN	>0.29
HER2-enriched– TN	<0.04*

Note: All significance values have been adjusted by Bonferroni correction for multiple comparisons. * p < .05. TN: Triple negative, HER2: human epidermal growth factor receptor 2.

3.4. Binary logistic regression and neural network performance for breast cancer

Our multivariable logistic regression and neural network analysis included age, diameter, and F/L index as independent variables in the model (Table 6). Regarding the binary logistic regression analysis, we developed a receiver operating characteristic curve (ROC) and obtained an Area Under the Curve (AUC) of 0.893, sensitivity of 79.63%, and specificity of 87.62%. Neural network analysis had similar outcomes with an AUC value of 0.903, sensitivity of 80.56%, and specificity of 88.57%. Both results were significant, with a p < 0.0001. The normalized importance of the independent variables was calculated as follows: age at 2.4%, diameter at 27.9%, and F/L index at 100%. Further, the cut-off value for the F/L index was >5.7, with a sensitivity and specificity of 84.26%. (Figure 5)

Table 6. Binary Logistic Regression Coefficients.

	Estimate	Standard Error	Odds Ratio	z	Wald Test			95% CI	
					Wald Statistic	df	p	Lower bound	Upper bound
Age	-0.05	0.01	0.95	-6.22	38.68	1	<.001	-0.07	-0.04
F/L INDEX	0.40	0.06	1.48	6.38	40.65	1	<.001	0.27	0.52
Diameter	0.01	0.01	1.01	0.49	0.24	1	0.62	-0.02	0.03

Note. Biopsy level 'POSITIVE' is coded as class 1. CI: Confidence interval, df: degrees of freedom.

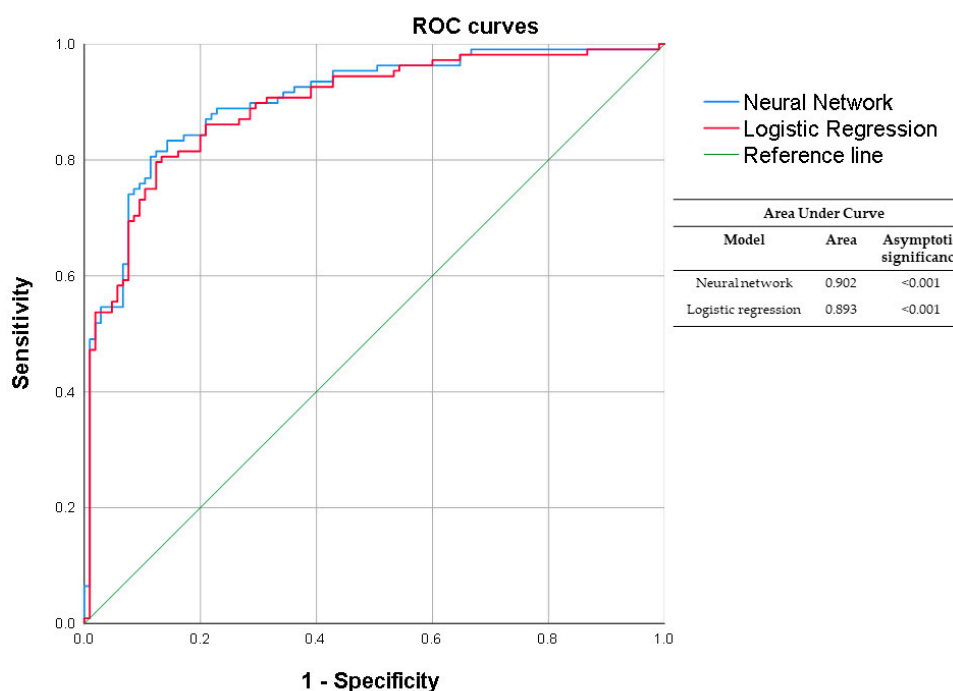


Figure 5. ROC curve comparing neural network versus logistic regression. The neural network performs 0.902 of AUC with a $p < 0.001$; Logistic regression shows an AUC of 0.893 and a $p < 0.001$.

4. Discussion

This manuscript reports the relationship between the F/L index, molecular subtypes of BC, and clinical stages of BC. An essential element distinguishing this work from previous publications on strain elastography was that the patients were matched by age.

Some research has focused on relating the F/L index with the molecular subtype and clinical stage of BC; recent publication of Zhu et al. [21] uses B mode US, real-time strain elastography (RTE), color doppler flow imaging (CDFI) and contrast-enhanced ultrasound (CEUS), those techniques were applied in 85 patients with histological BC and their molecular subtypes, ultrasound RTE and CDFI was significant in the binary logistic regression analysis ($p < 0.001$ and $p = 0.036$ respectively) for predictive Luminal A molecular subtype BC; for Luminal B, ultrasound RTE and CEUS showed a $p = 0.016$ and $p = 0.036$, respectively. Meanwhile, only CEUS discriminates HER2-enriched from other subtypes ($p = 0.039$); for the triple negative BC subtype (TNBCs), only CDFI ($p = 0.002$) obtained significant differences compared to TNBCs. Authors conclude that ultrasound RTE is affordable for Luminal subtypes, and CDFI and CEUS techniques are beneficial for measuring hypovascularity and hypervascularity, particularly in TNBCs and Luminal B breast tumors. In this sense, our findings agree with Zhu et al. in establishing a significant difference between several molecular subtypes; our research agrees that TNBCs were the softest tumors. Regarding the Luminal tumors, Luminal A had the most stiffness, similar to our study. However, in our research, the HER2-enriched was the hardest tumor among the rest of the tumors, unlike Zhu et al., who reported the Luminal A as the hardest tumor.

On the other hand, Hayashi et al. in 2015 [22] conducted an observational, retrospective study involving 503 patients with invasive BC, also considering clinicopathological features like molecular subtype BC, tumor size, invasive tumor size, lymph node metastasis, nuclear grade, age, menopausal status, BMI and breast density according to BI-RADS, they studied a subsample of 164 patients with frozen tissue, and they determined stroma-related gene expressions; they found clinical tumor stiffness correlated with lymph node involvement ($p = 0.0005$) and invasive tumor size ($p < 0.0001$), in the same study, multivariable analysis showed stiffness of primary breast tumor correlated with axillary lymph node metastasis as independent factor. Finally, respecting gene expression, they

report a higher expression of lysyl oxidase in hard tumors with FDR-adjusted $p=0.0279$, suggesting that the extracellular matrix plays a vital role in the etiology of tumor stiffness. Though we did not study the same variables as Hayashi et al., we obtained a similar correlation between tumor size and the F/L index, which means that the larger the size, the greater the hardness of the tumor ($r=0.35$, $p<0.001$) when all tumors are analyzed together regardless of molecular subtype.

Jin et al. [23] 2017 investigated SE and its relationship with tumor pathology, and tumor stiffness was determined regarding elasticity score and stiffness index. Jin et al. included 291 patients with invasive BC; they found 79% of tumors with a high stiffness index, and the average percentage of hardness was $82.32\pm 15.72\%$. The statistical analysis found a relationship between hardness with histological grade and molecular subtypes: grade I-II tumors were harder than grade III tumors, and Luminal A was harder than Luminal B, HER2-enriched, and the TNBCs. There was no relationship with histologic lineage or type. When contrasted with our findings, we found similarly that the Luminal A was one of the subtypes with higher hardness, but in our case, we found the HER2-enriched with higher hardness than Luminal A; this may be because there are few HER2-enriched tumors analyzed in both studies and the populations studied are different, which could lead to different results. However, what we did not confirm in our analysis in comparison with Jin et al. was the relationship of hardness with the degree of differentiation; this may be because we only included 2 cases with grade I, which might reduce the power of the study concerning this variable.

One of the most extensive studies about elastography and the F/L index is that of Togawa et al. [24]; this research group studied 1288 women with BIRADS 3 and 4a-4c through B-mode US, and SWE was evaluated with the F/L index. The F/L values were contrasted with the biopsy. These authors found 368 (28.6%) malignant tumors; after evaluation with conventional B-mode US 53.8% of benign lesions by biopsy were classified as BI-RADS 4, which corresponds to false positives; on the other hand, after US evaluation, they only classified 1.39% as BIRADS 3, but that upon biopsy were positive (false negatives). Our findings show similar results; however, 66.66% of benign biopsies at our site were classified as BI-RADS 4a-4c (false positives). We hypothesized that this divergence in results could be attributable because Togawa et al. used SWE, which is different from ours. Also, the population is ethnically diverse, and it is known that the breast tissue composition is different between Caucasian and Asian populations; it is worth mentioning that the Mexican population has an important ancestry of Asian migrants [25,26].

Last year, Lee et al. [27] investigated how fibrotic focus (FF) affects the SE in 151 patients with BC (46.9%) of patients were positive for FF, nevertheless were not significant with SE, with $p=0.633$; the rest of results have congruence with the reports previous in other manuscripts, they found statistics significance corresponding to clinical characteristics vs. positive SE like older age ($p=0.044$), larger tumors ($p=0.004$), and only clinical stage II vs. stage I and III they obtain a ($p=0.028$). This study proves that clinicopathological characteristics are correlated with the stiffness of the tumor and poor prognostic features of BC. According to our research, we do not evaluate fibrotic focus. However, similar to Lee et al., we found a correlation between F/L index with age and diameter of tumor ($p<0.0001$), as well as clinical stage of BC and BI-RADS into Spearman's correlation coefficient with $r=0.25$, it should be noted that we include BC stage IV because educational status in women in Mexico and Latin-American impacts stage at diagnosis of BC and unfortunately mostly of patients are diagnosed in stage III and IV.

As well as Çoraplı et al. [28] Recently, they intended to establish a correlation between SE and molecular subtypes of BC; however, they reported insignificant results in a total of 195 patients and concluded that SE is inefficient for identifying molecular subtypes of BC. Nonetheless, our results showed significance between Luminal A s. TN with $p<0.005$ and HER2 -enriched vs. TN $p<0.004$, possibly due to pairing patients.

In 2022, Shehata et al. [29] evaluated the performance of ultrasound elastography score (ES), quantitative mass strain ratio (SR), and shear wave elasticity ratio (SWE) in discerning between benign and malignant tumors. The study enrolled 51 patients; 77 histological breast masses were obtained, of which 57 tested positive for malignancy and 20 tested negatives for malignancy. As for SR, they reported a statistical difference between positive and negative biopsy ($p<0.001$);

furthermore, the cut-off value set for SR was >4.6 with a sensitivity of 96.5% and specificity of 80%. These results are consistent with our study. Shehata emphasizes that semi-quantitative elastography assessed by the F/L index is more objective than other methodologies for stiffness measurement, as it considers the patient's tissue as a reference. Thus, the relative reference to a non-tumor tissue is essential for an adequate prediction.

Finally, a systematic review of the meta-analysis of Mutala et al. [30] reported that the sensitivity and specificity for a cut-off point of 2.81 were 0.86 and 0.74, respectively. However, they warn about the importance of the functionality of the imaging tool and the need to consider that sonoelastography with its SR value makes sense when considering a previous breast exploration to characterize the type of lesion and the manufacturer model of the device.

5. Conclusions

Understanding the significance of SE and the application of F/L cut-off points can improve the diagnostic capability of mammography to reduce the proportion of false negatives and false positives in the diagnosis of breast cancer, as well as provide insight into the expected biological behavior concerning tissue hardness, clinical stages, and molecular phenotypes.

Author Contributions: Conceptualization, J.A.C.R.; G.C.L.A.; and M.I.T.C. methodology, L.A.G.V.; M.T.T.D and K.R.C.M.; formal analysis, J.A.C.R.; data curation, I.A.V.H.; writing—original draft preparation, J.A.C.R and G.C.L.A.; writing—review and editing, E.M.J.; project administration, E.M.J. All authors have read and agreed to the published version of the manuscript.

Funding: This research received no external funding.

Institutional Review Board Statement: This study was sustained following the regulations of the General Health Law, the Regulations of the General Health Law on Health Research, the guidelines established by COFEPRIS, the Health Law of the State of Jalisco, the Ethics and Research Committee of the OPD of IJC with number register CONBIOETICA-14-CEI-004-20170421, and those established by the E6 Good Clinical Practice (GCP) Guide of the International Conference on Harmonization (ICH).

Informed Consent Statement: Informed consent was obtained from all subjects involved in the study. All the patients gave written informed consent.

Acknowledgments: We are deeply grateful to Domitila Esparza Tostado for being a technical assistant in the radiology department and Beatriz Alejandra Llanes Cervantes for graphics and translation assistance for this study.

Conflicts of Interest: The authors declare no conflict of interest.

References

1. WORLD HEALTH ORGANIZATION GLOBAL CANCER OBSERVATORY. *CANCER TODAY*.
2. Ormachea, J.; Parker, K.J. Elastography Imaging: The 30 Year Perspective. *Phys Med Biol* **2020**, *65*, doi:10.1088/1361-6560/abca00.
3. Doyley, M.M.; Parker, K.J. Elastography: General Principles and Clinical Applications. *Ultrasound Clin* **2014**, *9*, 1–11, doi:10.1016/j.cult.2013.09.006.
4. Sigrist, R.M.S.; Liau, J.; Kaffas, A.E.; Chammas, M.C.; Willmann, J.K. Ultrasound Elastography: Review of Techniques and Clinical Applications. *Theranostics* **2017**, *7*, 1303–1329, doi:10.7150/thno.18650.
5. Chee, C.; Lombardo, P.; Schneider, M.; Danovani, R. Comparison of the Fat-to-Lesion Strain Ratio and the Gland-to-Lesion Strain Ratio With Controlled Precompression in Characterizing Indeterminate and Suspicious Breast Lesions on Ultrasound Imaging. *J of Ultrasound Medicine* **2019**, *38*, 3257–3266, doi:10.1002/jum.15037.
6. Zhi, H.; Xiao, X.-Y.; Yang, H.-Y.; Wen, Y.-L.; Ou, B.; Luo, B.-M.; Liang, B. Semi-Quantitating Stiffness of Breast Solid Lesions in Ultrasonic Elastography. *Academic Radiology* **2008**, *15*, 1347–1353, doi:10.1016/j.acra.2008.08.003.
7. Franco Uliaque, C.; Pardo Berdún, F.J.; Laborda Herrero, R.; Pérez Lórenz, C. Utilidad de la elastografía semicuantitativa para predecir la malignidad de los nódulos tiroideos. *Radiología* **2016**, *58*, 366–372, doi:10.1016/j.rx.2016.05.001.
8. Barr, R.G. Future of Breast Elastography. *Ultrasonography* **2019**, *38*, 93–105, doi:10.14366/usg.18053.

9. Sandrin, L.; Fourquet, B.; Hasquenoph, J.-M.; Yon, S.; Fournier, C.; Mal, F.; Christidis, C.; Ziol, M.; Poulet, B.; Kazemi, F.; et al. Transient Elastography: A New Noninvasive Method for Assessment of Hepatic Fibrosis. *Ultrasound Med Biol* **2003**, *29*, 1705–1713, doi:10.1016/j.ultrasmedbio.2003.07.001.
10. Fang, C.; Huang, D.Y.; Sidhu, P.S. Elastography of Focal Testicular Lesions: Current Concepts and Utility. *Ultrasonography* **2019**, *38*, 302–310, doi:10.14366/usg.18062.
11. Zhao, C.-K.; Xu, H.-X. Ultrasound Elastography of the Thyroid: Principles and Current Status. *Ultrasonography* **2019**, *38*, 106–124, doi:10.14366/usg.18037.
12. Yilmaz, E.; Yilmaz, A.; Aslan, A.; Inan, I.; Evren, M.C.; Tekesin, K. Real-Time Elastography for Differentiation of Breast Lesions. *Pol J Radiol* **2017**, *82*, 664–669, doi:10.12659/PJR.902596.
13. ELMowalled, S. Value of Ultrasound Elastography in Combined with Mammography in Evaluation of Indeterminate Breast Lesions. *Benha Journal of Applied Sciences* **2023**, *0*, 0–0, doi:10.21608/bjas.2023.195843.1093.
14. Mendelson, E.; Böhm-Vélez, M.; Berg, W. 2013.
15. You, Y.; Song, Y.; Li, S.; Ma, Z.; Bo, H. Quantitative and Qualitative Evaluation of Breast Cancer Prognosis: A Sonographic Elastography Study. *Med Sci Monit* **2019**, *25*, 9272–9279, doi:10.12659/MSM.918806.
16. Barr, R.G.; Nakashima, K.; Amy, D.; Cosgrove, D.; Farrokh, A.; Schafer, F.; Bamber, J.C.; Castera, L.; Choi, B.I.; Chou, Y.-H.; et al. WFUMB Guidelines and Recommendations for Clinical Use of Ultrasound Elastography: Part 2: Breast. *Ultrasound in Medicine & Biology* **2015**, *41*, 1148–1160, doi:10.1016/j.ultrasmedbio.2015.03.008.
17. Niknejad, M.; Weerakkody, Y. Breast Imaging-Reporting and Data System (BI-RADS). In *Radiopaedia.org*; Radiopaedia.org, 2010.
18. Gnant, M.; Harbeck, N.; Thomssen, C. St. Gallen 2011: Summary of the Consensus Discussion. *Breast Care* **2011**, *6*, 136–141, doi:10.1159/000328054.
19. Thomssen, C.; Balic, M.; Harbeck, N.; Gnant, M. St. Gallen/Vienna 2021: A Brief Summary of the Consensus Discussion on Customizing Therapies for Women with Early Breast Cancer. *Breast Care* **2021**, *16*, 135–143, doi:10.1159/000516114.
20. Giuliano, A.E.; Edge, S.B.; Hortobagyi, G.N. Eighth Edition of the AJCC Cancer Staging Manual: Breast Cancer. *Ann Surg Oncol* **2018**, *25*, 1783–1785, doi:10.1245/s10434-018-6486-6.
21. Zhu, J.-Y.; He, H.-L.; Jiang, X.-C.; Bao, H.-W.; Chen, F. Multimodal Ultrasound Features of Breast Cancers: Correlation with Molecular Subtypes. *BMC Med Imaging* **2023**, *23*, 57, doi:10.1186/s12880-023-00999-3.
22. Hayashi, M.; Yamamoto, Y.; Sueta, A.; Tomiguchi, M.; Yamamoto-Ibusuki, M.; Kawasoe, T.; Hamada, A.; Iwase, H. Associations Between Elastography Findings and Clinicopathological Factors in Breast Cancer. *Medicine* **2015**, *94*, e2290, doi:10.1097/MD.0000000000002290.
23. Jin, Y.; Fenghua, L.; Jing, D.; Yifen, G. Strain Elastography Features in Invasive Breast Cancer: Relationship between Stiffness and Pathological Factors. *Int J Clin Exp Med* **2017**, *10*, 13290–13297.
24. Togawa, R.; Pfob, A.; Büsch, C.; Alwafai, Z.; Balleyguier, C.; Clevert, D.; Duda, V.; Fastner, S.; Goncalo, M.; Gomez, C.; et al. Potential of Lesion-to-Fat Elasticity Ratio Measured by Shear Wave Elastography to Reduce Benign Biopsies in BI-RADS 4 Breast Lesions. *J of Ultrasound Medicine* **2023**, *42*, 1729–1736, doi:10.1002/jum.16192.
25. Patel, B.K.; Pepin, K.; Brandt, K.R.; Mazza, G.L.; Pockaj, B.A.; Chen, J.; Zhou, Y.; Northfelt, D.W.; Anderson, K.; Kling, J.M.; et al. Association of Breast Cancer Risk, Density, and Stiffness: Global Tissue Stiffness on Breast MR Elastography (MRE). *Breast Cancer Res Treat* **2022**, *194*, 79–89, doi:10.1007/s10549-022-06607-2.
26. Rodríguez-Rodríguez, J.E.; Ioannidis, A.G.; Medina-Muñoz, S.G.; Barberena-Jonas, C.; Blanco-Portillo, J.; Quinto-Cortés, C.D.; Moreno-Estrada, A. The Genetic Legacy of the Manila Galleon Trade in Mexico. *Phil. Trans. R. Soc. B* **2022**, *377*, 20200419, doi:10.1098/rstb.2020.0419.
27. Lee, N.-R.; Oh, H.-K.; Jeong, Y.-J. Clinical Significance of Ultrasound Elastography and Fibrotic Focus and Their Association in Breast Cancer. *JCM* **2022**, *11*, 7435, doi:10.3390/jcm11247435.
28. Çoraplı, M.; Bulut, H.T.; Örmeci, A.G.; Alakuş, H. Relationship between Strain Elastography and Histopathological Parameters in Breast Cancer. *Cukurova Medical Journal* **2022**, *47*, 1663–1669, doi:10.17826/cumj.1131781.
29. Shehata, R.M.A.; El-Sharkawy, M.A.M.; Mahmoud, O.M.; Kamel, H.M. Qualitative and Quantitative Strain and Shear Wave Elastography Paradigm in Differentiation of Breast Lesions. *Egyptian Journal of Radiology and Nuclear Medicine* **2022**, *53*, 23, doi:10.1186/s43055-022-00697-0.
30. Mutala, T.M.; Mwangi, G.N.; Aywak, A.; Cioni, D.; Neri, E. Determining the Elastography Strain Ratio Cut off Value for Differentiating Benign from Malignant Breast Lesions: Systematic Review and Meta-Analysis. *Cancer Imaging* **2022**, *22*, 12, doi:10.1186/s40644-022-00447-5.

Disclaimer/Publisher's Note: The statements, opinions and data contained in all publications are solely those of the individual author(s) and contributor(s) and not of MDPI and/or the editor(s). MDPI and/or the editor(s) disclaim responsibility for any injury to people or property resulting from any ideas, methods, instructions or products referred to in the content.